IOP Conf. Series: Materials Science and Engineering **192** (2017) 012027 doi:10.1088/1757-899X/192/1/012027

Computation material science of structural-phase transformation in casting aluminium alloys

V M Golod[1] and L Yu Dobosh[1,]

[1]Peter the Grate St.Petersburg Polytechnic University, Institute of Metallurgy, Mechanical Engineering and Transport, Department of Metallurgical and Casting Technologies, 195251, Saint-Petersburg, Russia

E-mail: lpi2015@mail.ru

Abstract. Successive stages of computer simulation the formation of the casting microstructure under non-equilibrium conditions of crystallization of multicomponent aluminum alloys are presented. On the basis of computer thermodynamics and heat transfer during solidification of macroscale shaped castings are specified the boundary conditions of local heat exchange at mesoscale modeling of non-equilibrium formation the solid phase and of the component redistribution between phases during coalescence of secondary dendrite branches. Computer analysis of structural - phase transitions based on the principle of additive physico-chemical effect of the alloy components in the process of diffusional - capillary morphological evolution of the dendrite structure and the o of local dendrite heterogeneity which stochastic nature and extent are revealed under metallographic study and modeling by the Monte Carlo method. The integrated computational materials science tools at researches of alloys are focused and implemented on analysis the multiple-factor system of casting processes and prediction of casting microstructure.

1. Introduction

Reliable technology foresight of casting technology for manufacturing high-quality products, as well as for the successful synthesis of casting alloys with the desired structure and properties is provided by the development of adequate mathematical models produced in the field of ***computational thermodynamics*** (CTD) and ***computational heat transfer*** (CHT) for the analysis of the conditions of solidification of castings, also on the basis of ***computational materials science*** models (CMS) in order to predict the processes of formation of the microstructure of multicomponent alloys with a dendritic morphology that can be integrated into the modern theory of casting processes.

2. Problems and prospects of CTD models implementation

Using a number of specialized software systems (FactSage - since 1976, ThermoCalc - since 1981, Polytherm - since 2000, etc.) allows to implement in technological developments the powerful mathematical models of equilibrium thermodynamic analysis of phase transformations of various physico-chemical nature. These models should reflect the crystalline structure of alloys and processes occurring during phase transitions, taking into account the redistribution of components between phases, as well as the composition and amount of solid phase under equilibrium and non-equilibrium crystallization of stable and metastable phases. The mathematical apparatus of CTD for metal systems

is based on a universal model of subregular solutions used for quantitative description of the physico-chemical processes under the phase transformations based on the synthesis of metal physics, materials science and computer technology [1-3].

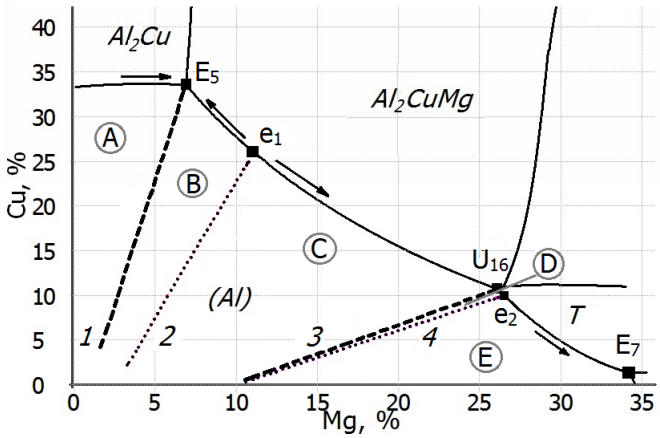

Figure 1. Areas (A-E) formation of various structural components and the corresponding dividing lines (*1-4*) under crystallization of Al-Cu-Mg alloys.

Figure 1 shows the calculated fragment of liquidus surface for ternary system Al-Cu-Mg [4], indicating areas and boundaries of areas of the various structural components, which is the basis for modeling of its crystallization. Modeling of phase transformation provides the ability to calculate the temperature functions for coefficients $k(t)$ and $p(t)$, which is dictated by the considerable scale of the it's changes taking place during the crystallization (figure 2.) - from 30 to 70-90%. The appropriate correction of algorithm of used CTD software allows to calculate the course of phase transformation not only under equilibrium conditions, but also at the complete suppression of diffusion in the solid phase (Scheil model) [3-5], including the fraction of the releasing phases, temperature functions of specific heat of phases $c_m(t)$ and the latent heat of crystallization $L_m(t)$.

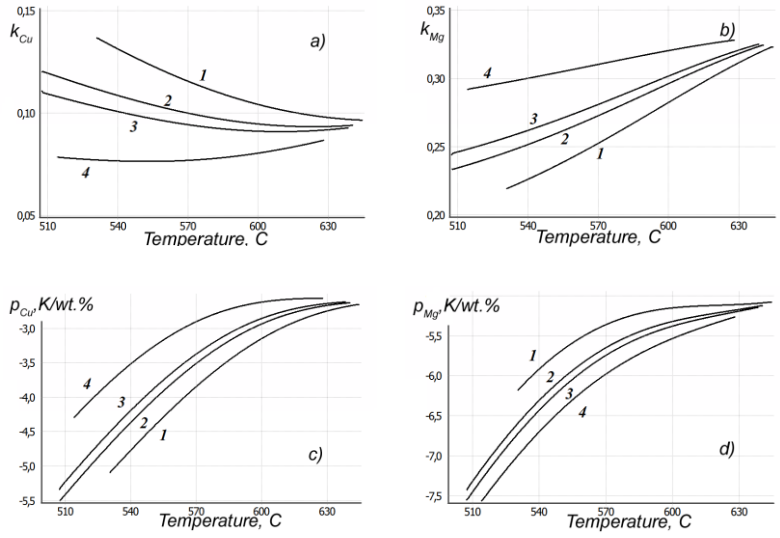

Figure 2. Effect of the composition of alloys Al - 4,5% Cu - Mg on changing the distribution coefficients k_{Cu} (*a*)- k_{Mg} (*b*) and slope of liquidus p_{Cu} (c) - p_{Mg} (d) in the temperature range of equilibrium crystallization of the primary solid phase α-Al at Mg,% = 0.8 (*1*); 1.6 (*2*); 2.0 (*3*); 4.0 (*4*).

Further development of tools and experimental techniques CTD will eliminate the existing at the moment a significant (up to 5-10 wt.%) number of mismatching lines and critical points, delimiting the phases formation region (including - for the most important systems on the basis of iron and aluminum) [5], as well as realization of the thermodynamic support users of a certain group of alloys (silumins, tin bronzes, stainless steels, etc.), for which a

local adaptation of a computational thermodynamic model can be made cheaper and more accurate.

3. The multi-level synthesis of CHT tools

The analysis of the complex processes that occur during the formation of the casting of any configuration is carried out by generation for the macrosystem the net of small mesoelements, which are characterized by a uniform temperature distribution (the grid number of Bi << 1) and the concentration of residual melt. Solution the problem of casting solidification is based on the analysis of its heat exchange with the environment – the mold or ingot (figure 3), which is described by the Fourier equation:

$$c_m \frac{\partial t}{\partial \tau} = \lambda_m \nabla^2 t + \frac{\partial Q_m}{\partial \tau}, \qquad (1)$$

where τ – time; c_m, Q_m, λ_m – volumetric heat capacity, heat of crystallization and thermal conductivity of the alloy. For further solution it is necessary to define the initial and boundary conditions of heat transfer and thermal properties of materials [3].

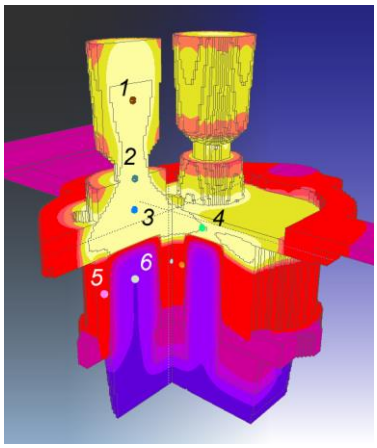

Figure 3. Distribution of temperature during the casting solidification (alloy AK12, weight - 45 *kg*) in sand mold with registration the local heat transfer conditions in the control points of casting (*1-5*) and mould (*6*).

After splitting the macro-object by spatial grid with a increments $\Delta x \times \Delta y \times \Delta z$ for three coordinate axes the calculation of the effective heat flux for the *i*-th selected mesoelement of the three-dimensional geometric macromodel is based on the local heat balance equation:

$$q_i = \left(\frac{V_i}{F_i}\right)\frac{Q_m}{(\tau_{LS})_i} = \frac{R_i Q_m}{(\tau_{LS})_i}, \qquad (2)$$

where the value of q_i is to be defined by averaging the results of numerical calculation of heat transfer in the modeling of solidification by time τ_{LS} for mesoelement, which is selected for the purpose of local analysis of the crystallization process in a given domain of R_i size.

Dataware for heat calculation of casting solidification, based on thermodynamic modeling of phase transformation of alloy involves the additional determination of the temperature functions of the density $\rho_m(t)$ and the thermal conductivity $\lambda_m(t)$, which is defined by generalizing of known experimental data using neural network models [6], as well as their diffusion coefficients in liquid D_L and solid D_S phase. Thermal properties of the moulding materials $c_f(t)$ and $\lambda_f(t)$, which technological characteristics are caused by grain and mineralogical composition, humidity of mixture and its degree of compaction is determined by computer-automated procedure for solving the inverse problem based on data of thermal analysis of mould heating during the solidification test of experimental sample [6].

4. Mesoscale model of non-equilibrium releasing of the solid phase

Progress of the non-equilibrium crystallization of multi-component (i = 2, ... K) alloy describes the system (3a-3c) which interconnected the changes in the concentration of the components in melt, fraction of the released primary solids phase $m(t)$ and temperature $t(\tau)$ [7-*8*]:

$$\begin{cases} \dfrac{dC_i^L}{dm} = \dfrac{C_i^L(1-k_i)}{1-m(1-\sigma_i k_i)}; \quad \text{(a)} \\ \dfrac{dm}{dt} = \dfrac{1}{\sum\limits_2^K \dfrac{p_i C_i^L(1-k_i)}{1-m(1-\sigma_i k_i)}}; \quad \text{(b)} \\ qd\tau = -Rc_m dt + RL_m dm, \quad \text{(c)} \end{cases} \tag{3}$$

where $\sigma_i = 2\alpha_i/(1+2\alpha_i)$; $\alpha_i = 8D_i^S \tau_{LS}/\lambda_2^2$ [9] – the degree of suppression of diffusion in the solid phase, estimated on the basis of adjacent calculation of secondary dendrite arm spacing $\lambda_2(\tau)$ of the primary solids phase.

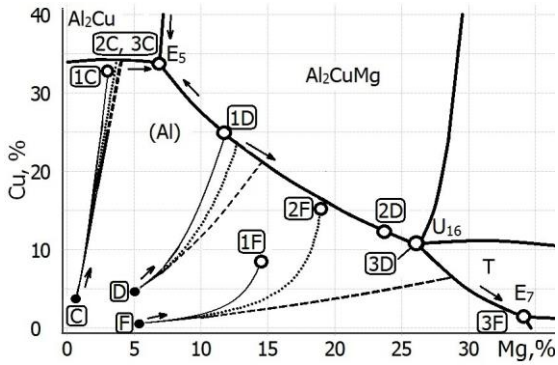

Figure 4. Solidification paths of *C*, *D* and *F* alloys on the liquidus surface of ternary system Al-Cu-Mg at various intensity of diffusion in the solid phase:
$D_i^S = \infty$; $\sigma_i = 1$ (*1*);
$\infty > D_i^S > 0$; $1 > \sigma_i > 0$ (*2*);
$D_i^S = 0$; $\sigma_i = 0$ (*3*).

The paths of crystallization of various alloys (figure 4) with similar initial composition (0.5-5% Cu; 1-5% Mg) demonstrate the radical difference of the trajectories and the final reached structure (the fractions and compositions of the resulting eutectic - E_5, U_{16} or E_7), depending on the diffusion conditions in solid phase and the morphology of the dendritic structure that has a significant influence on the course of the casting processes and the mechanical properties of the alloy. The results of numerical calculation using system of non-equilibrium models (3a - 3c) for estimating the rate of primary solid phase formation (figure 5) and changing the composition of the liquid phase (figure 6) are compared with the data of thermodynamic calculation (CTD) under equilibrium conditions ($D_S = \infty$) and complete suppression of diffusion in the solid phase ($D_S = 0$ - Scheil model).

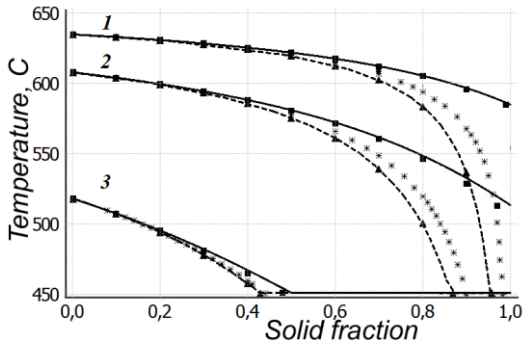

Figure 5. Changes temperature of Al-Mg alloy with 5 (*1*), 10 (*2*) and 25 (*3*)% Mg under different crystallization conditions: lines - CTD, $D_S = \infty$; dotted lines - CTD, $D_S = 0$; points - system of models (3a-3c) for $\sigma = 1.0$ (■); $\sigma = 0{,}5$ (*); $\sigma = 0.0$ (▲).

Evident coincidence between the numerical calculation results according to the system of models (3), presented in figure 5-6 by points, with CTD data under the same assumptions ($\sigma = 1.0$ and $\sigma = 0.0$)

indicates the adequacy of both system components – (3a) and (3b), and the possibility of their use for predicting the phase transformation.

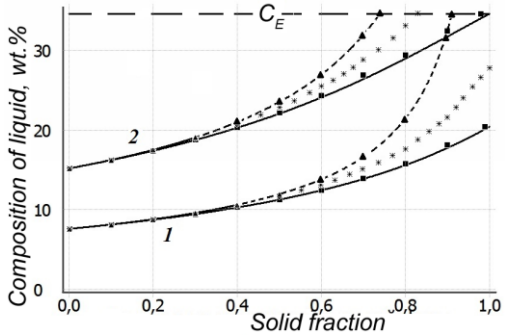

Figure 6. Changes of liquid phase composition of Al-Mg alloy with 8 (*1*) and 15 (2)% Mg under different crystallization conditions: lines - CTD, $D_S = \infty$; dotted lines - CTD, $D_S = 0$; points - system of models (3a-3c) for σ = 1.0 (■); σ = 0,5 (*); σ = 0.0 (▲).

An important feature of the above systems of models (3a-3c) is the using in the modeling of principles: *independent* action of intra-phase and inter-phase diffusion of components (3a - model) and *additive* influence of components on rate of formation of the solid phase (3b - model) with account the dependence from temperature of thermodynamic (*p*, *k*) and kinetic (D_i^S) parameters.

5. Mesoscale model of dendritic structure evolution

Mesoscale equiaxed crystallization of multicomponent alloys develop step-by-step by formation the solid phase during the creation and growth of the ensemble of dendritic crystallites in *interdendritic* melt up to their closing (first stage) followed by capillary-diffusion coalescence in the volume of *intradendritic* liquid phase (second stage) under the influence of the Gibbs-Thomson effect. The initial process of formation of dendrite in the period of maximum supercooling of the melt and its subsequent recalescence leads to origination the ensemble of differently oriented and non-uniformly distributed secondary branches that differ significantly in length, diameter and curvature of the surface in array with a variety of dendrite arm spacing λ_0 [10]. The dendritic morphology, formed during the evolution of the primary non-homogeneous massif during a competitive implementation of various coalescence mechanisms [11], leads to a continuous increase the average size of the secondary dendrite space $\lambda_2(\tau)$ and their scope $\sigma_\lambda(\tau)$ up to the moment of exhaustion of intradendritic liquid phase at $\tau = \tau_{LS}$.

The course of evolution of the dendritic structure, evaluated by changes in the most important parameter – averaged $\lambda_2(\tau)$, describes an equation based on a generalized model [12]:

$$\frac{d(\lambda_2^3)}{d\tau} = \frac{1}{\varphi_j \sum_K \frac{p_i(1-k_i)C_i^L}{\Gamma_i D_i^L}}, \qquad (4)$$

where Γ_i – Gibbs-Thomson coefficient for the *i*-th component of the alloy, φ_j – adopted rate of coalescence mechanism. Analysis of a large array of experimental data (more than 110, R=0.98) of the averaged (finite) values of secondary dendritic spacing λ_K for binary and ternary aluminum alloys (figure 7) in comparison with the calculation on the equation (4) allow to carry out its statistical calibration and set the effective value of the coefficient φ for alloys of different composition, established the predominant mechanism of coalescence – radial dissolution/thickening of the branches ($\varphi \approx \varphi_{II}$ [12]).

The set of equations (3) and (4) forms a system model ALSYS [16], which allows to consider quantitatively the relationships of physical and chemical nature in the course of consistent non-equilibrium crystallization of multicomponent aluminum alloys and reveal the influence of thermodynamic, thermal, diffusion and capillary factors on the morphology and volume fraction of the dendrite structure (with further modeling of the second stage of alloys crystallization – formation of binary and ternary eutectics).

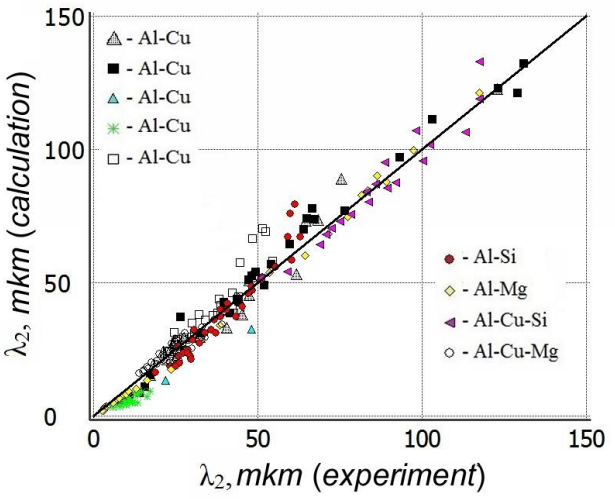

Figure 7. Comparison of calculated and experimental values λ_2 [13-15 etc.] of binary and ternary aluminum alloys using after calibration testing the different coalescence models I-IV [12] respectively various φ for alloy groups: $\varphi_I \approx \varphi_{III}$ (Al-Cu); φ_{II} (Al-Cu-Si, Al-Si; Al-Mg);
φ_{IV} (Al-Cu-Mg).

Complex diagram of system modeling the characteristics of crystallization process of ternary alloy Al-5% Cu-5% Mg, shown in figure 8 for different conditions of the heat removal, shows the relationship of the time of successive stages of the crystallization process (τ_α, τ^b_E, τ^t_E), release kinetics and the fraction of solid phase (figure 8,a-b), the composition of the residual liquid phase (figure 8, c-d), as well as the intensity and completeness of diffusion processes (figure 8, e-f) and – as a result – the evolution of the parameters (λ_2, λ^b_E, λ^t_E) of the microstructure (figure 8, g) from the rate of cooling at different stages of solidification.

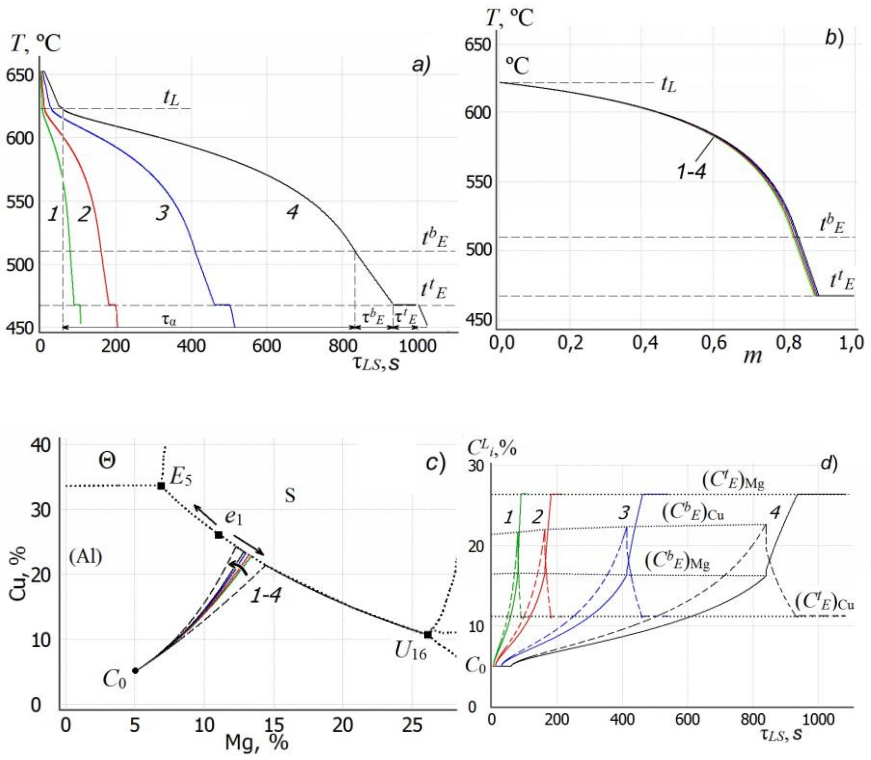

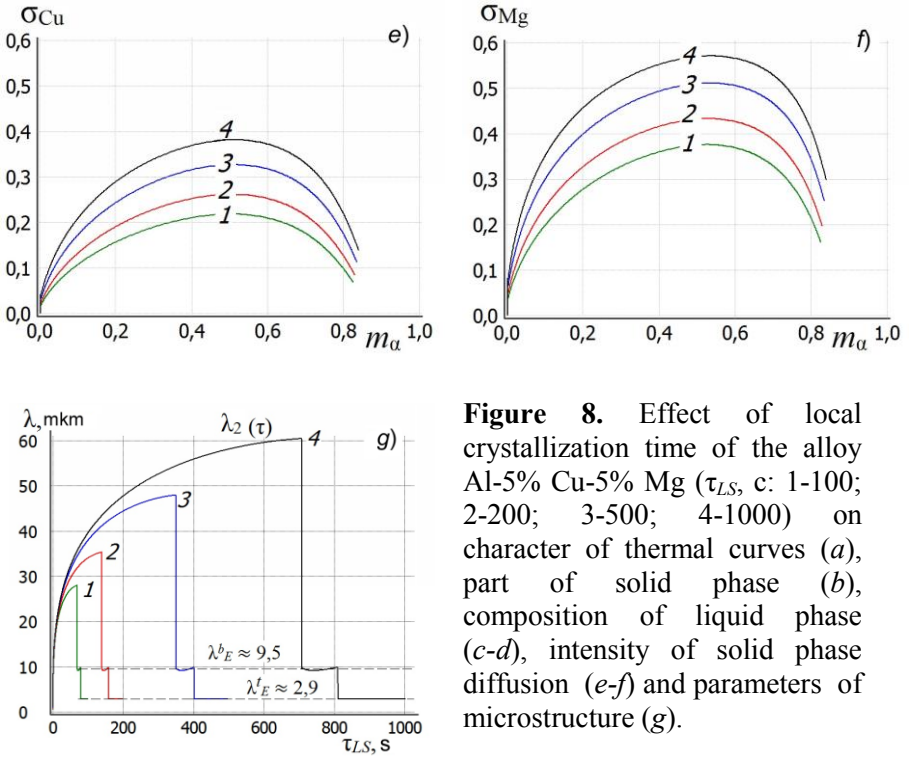

Figure 8. Effect of local crystallization time of the alloy Al-5% Cu-5% Mg (τ_{LS}, c: 1-100; 2-200; 3-500; 4-1000) on character of thermal curves (*a*), part of solid phase (*b*), composition of liquid phase (*c-d*), intensity of solid phase diffusion (*e-f*) and parameters of microstructure (*g*).

The adequacy of the system model to predict the dendritic structure confirmed by the results of metallographic control (figure 9), which shows a linearized dependence $\lambda_2=K\tau_{LS}^n$ of local solidification time τ_{LS} (in a wide range from 5.2 to 10^3s) for averaged values of dendrite arm spacing $(\lambda_2)_{av}$ of investigated cast samples.

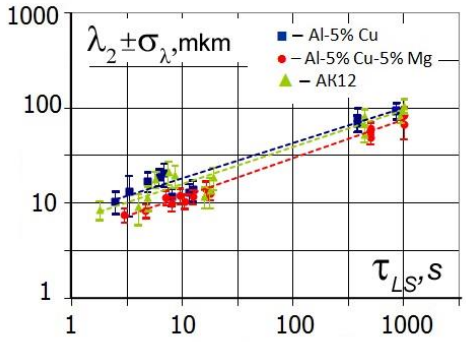

Figure 9. Dependence of the secondary dendrite spacing (averaged statistical data $(\lambda_2)_{av}$ $\pm\sigma_\lambda$ of microstructure studied on the cross section of the cast samples) for alloys Al-5% Cu, Al-5% Cu-5% Mg and AK12 from a local solidification time τ_{LS}.

The data obtained are characterized by similar values of exponents (n=0.37-0.40) at relatively high values of the correlation coefficient ($R\approx$0.94-0.98) and large scale of λ_2 values reaching 18-30% of $(\lambda_2)_{av}$.

6. Local inhomogeneity of the dendrite structure

The mentioned character of the inhomogeneity of the dendritic structure are represented by histograms distribution of end dendritic arm spacings (figure 10), which show significant local range on the scale of a separated dendrite and its nearest neighbors. This inhomogeneity of secondary arms caused by

intense coalescence, develops between the growing side branches with the cessation of growth and their dissolution on the interface area of increased curvature.

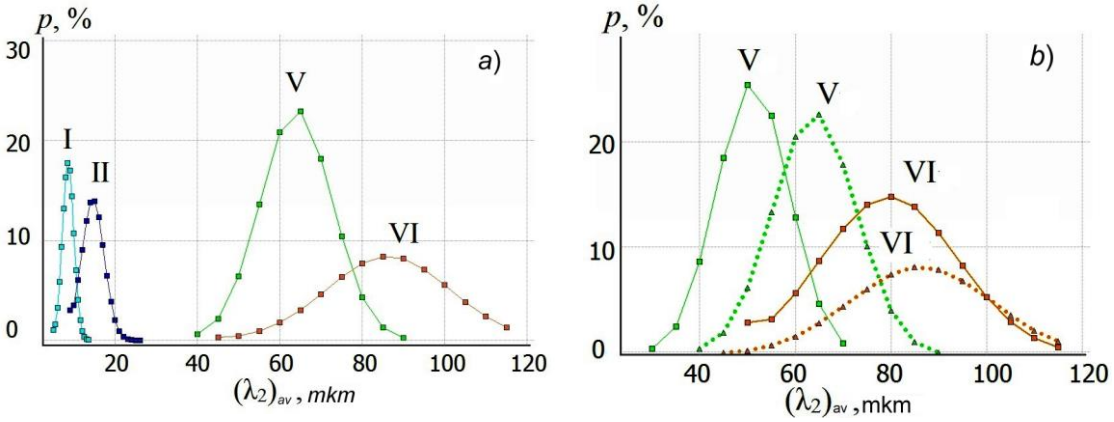

Figure 10. The frequency distribution of dendritic arm spacing in castings of different thicknesses (I-II: 10-15 mm; V-VI: 40-70 mm) in metal (I-II) or sand (V-VI) molds a) structure of axial zones; b) structure of surface (solid line) or centre (dotted line) zones.

Modeling the evolution of the dendritic structure was carried out using the Monte Carlo method [11] by calculation of competitive serial realization of various steps of coalescence in a statistical array with inhomogeneous distribution of morphological parameters of the crystallizing system [10]. Its result shows – in the accordance with experimental data (figure 10) – that the increasing of solidification and coalescence time causes growth of a mean value $(\lambda_2)_{av}$ and the limiting values $(\lambda_2)_{max}$ and $(\lambda_2)_{min}$ with sequential increase their scope, which is the driving force for repeated and continuous growth of these parameters.

7. Conclusion

System computer analysis of the inhomogeneous initial ensemble of secondary branches and its coalescence during crystallization shows that the stochastic processes of nucleation and evolution of dendritic branches in the interdendritic and intradendritic melt play a decisive role in shaping the final morphology and dispersity of the dendritic structure of alloys and non-equilibrium rate of releasing the solid phase under redistribution of components between the phases. The results of mesoscale analysis done in the framework of macroscale multi-dimensional configuration of the solidified casting (figure 3) allow to quantify the nature of the casting processes, that developed in the period of liquid to solid transformation for prediction the intensity and localization of casting defects [10].

8. References

[1] Hillert M and Staffanson L-I The regular solution model for stoichiomertric phases and ionic melts 1970 *Acta Chem. Scand.* **24** 3618-3626
[2] *Materials Modeling Series: SGTE bookcase. Thermodynamics* 1996 (London: Inst. of Materials)
[3] Golod V M, Savel'ev K D and Basin A S 2008 *Modeling and Computer Analysis of Crystallization of Multicomponent Iron-based Alloys* (Saint Petersburg: Polytechnic Univ Press)
[4] Golod V M, Savel'ev K D, Dobosh L Yu and Orlova I G 2014 Computational thermodynamics – the tool of foundry technology (review and forecast) *Metallurgy of Mechanical Engineering* **6** 27-33
[5] Golod V M and Savel'ev K D 2010 *Computational Thermodynamics in Materials Science* (Saint Petersburg Polytechnic Univ Press)

[6] Golod V M 2008 Computer analysis of foundry technology. Problems of its information support and adaptation to the conditions of production *Bull. Udmurt University: Physics. Chemistry* **1** 67-87
[7] Dobosh L Yu and Golod V M 2015 Prediction of microstructure parameters of ternary aluminum alloys on the basis of modeling non-equilibrium crystallization *Scientific and Technical Bull.* **3** 92-101
[8] Golod V M, Dobosh L Yu and Savel'ev K D 2014 Assessing the adequacy of the model of additive components influence on the crystallization of aluminum alloys *Proc. 10-th Int. Conf. Foundry today and tomorrow* 366-376
[9] Ohnaka J 1986 Mathematical analysis of solute redistribution during solidification with diffusion in solid phase *Trans. ISIJ* **26** 1045-1051
[10] Golod V M and Emel'yanov K I 2014 System analysis of morphological evolution of the dendritic steel structure *Ferrous Materials* **4** 49-54
[11] Golod V M, Emel'yanov K I and Orlova I G 2013 The dendritic heterogeneity of cast steel: an overview of problems and computer analysis (Part 3) *Ferrous Materials* **11** 18-25
[12] Han Q, Hu H and Zhong X 1997 Models for the isothermal coarsening of secondary dendrite arms in multicomponent alloys *Metall. Mater. Trans.* B **28** 1185-1187
[13] Bouchard D and Kirkaldy JS 1997 Prediction of dendrite arm spacings in unsteady and steady-state heat flow of unidirectionally solidified binary alloys *Metall. Mater. Trans. B* **28** 651-663
[14] Rodrigues J R P, Melo M L N M and Santos R G 2010 Effect of magnesium content on thermal and structural parameters of Al-Mg alloys directionally solidified *J. Mater. Sci.* **45** 2285-2295
[15] Berkdemir A and Gündüz M 2009 Effect of growth rate and Mg content on dendrite tip characteristics of Al–Cu–Mg ternary alloys *Appl. Phys. A* **96** 873-886
[16] Dobosh L Yu and Golod V M 2013 The influence of composition multicomponent aluminum alloys on the secondary arm spacing of dendrites *Foundryman of Russia* **3** 35-39